Article

Cell Reports

Zika Virus Infection in Mice Causes Panuveitis with Shedding of Virus in Tears

Graphical Abstract

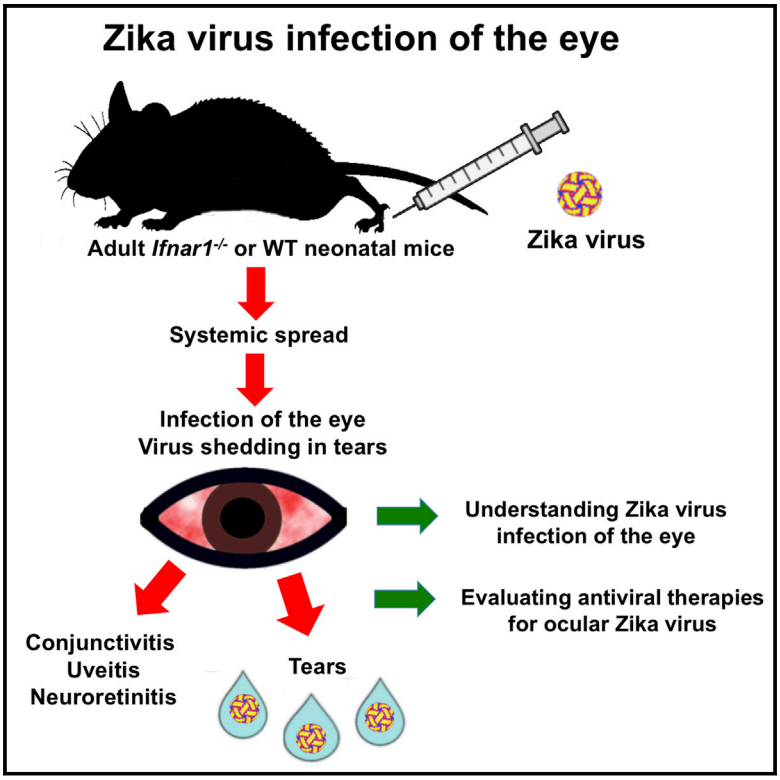

Highlights

- ZIKV infects several different regions of the eye, including the retina
- ZIKV RNA can be detected in tear fluid
- Eye and brain infection in adult mice by ZIKV occurs independently of the AXL receptor
- ZIKV infection results in apoptosis of neurons of the visual processing pathway

Authors

Jonathan J. Miner, Abdoulaye Sene, Justin M. Richner, ..., Gregory D. Ebel, Michael S. Diamond, Rajendra S. Apte

Correspondence

miner@wustl.edu (J.J.M.), diamond@borcim.wustl.edu (M.S.D.), apte@vision.wustl.edu (R.S.A.)

In Brief

Miner et al. now describe how ZIKV infection in the eye results in inflammation and injury. ZIKV infected the iris, cornea, retina, and optic nerve and caused conjunctivitis, panuveitis, and neuroretinitis in mice. This manuscript establishes a model for evaluating treatments for ZIKV infections in the eye.

Miner et al., 2016, Cell Reports *16*, 3208–3218
September 20, 2016
http://dx.doi.org/10.1016/j.celrep.2016.08.079

CellPress

OPEN ACCESS
CellPress

Cell Reports
Article

Zika Virus Infection in Mice Causes Panuveitis with Shedding of Virus in Tears

Jonathan J. Miner,[1,9,*] Abdoulaye Sene,[2,9] Justin M. Richner,[1] Amber M. Smith,[1] Andrea Santeford,[2] Norimitsu Ban,[2] James Weger-Lucarelli,[3] Francesca Manzella,[4] Claudia Rückert,[3] Jennifer Govero,[1] Kevin K. Noguchi,[4] Gregory D. Ebel,[3] Michael S. Diamond,[1,5,6,7,10,*] and Rajendra S. Apte[1,2,8,*]

[1]Department of Medicine
[2]Department of Ophthalmology and Visual Sciences
School of Medicine, Washington University, Saint Louis, MO 63110, US
[3]Department of Microbiology, Immunology and Pathology, College of Veterinary Medicine and Biomedical Sciences, Colorado State University, Fort Collins, CO 80523, USA
[4]Department of Psychiatry
[5]Department of Molecular Microbiology
[6]Department of Pathology and Immunology
[7]The Center for Human Immunology and Immunotherapy Programs
[8]Department of Developmental Biology
School of Medicine, Washington University, Saint Louis, MO 63110, USA
[9]Co-first author
[10]Lead Contact
*Correspondence: miner@wustl.edu (J.J.M.), diamond@borcim.wustl.edu (M.S.D.), apte@vision.wustl.edu (R.S.A.)
http://dx.doi.org/10.1016/j.celrep.2016.08.079

SUMMARY

Zika virus (ZIKV) is an emerging flavivirus that causes congenital abnormalities and Guillain-Barré syndrome. ZIKV infection also results in severe eye disease characterized by optic neuritis, chorioretinal atrophy, and blindness in newborns and conjunctivitis and uveitis in adults. We evaluated ZIKV infection of the eye by using recently developed mouse models of pathogenesis. ZIKV-inoculated mice developed conjunctivitis, panuveitis, and infection of the cornea, iris, optic nerve, and ganglion and bipolar cells in the retina. This phenotype was independent of the entry receptors Axl or Mertk, given that *Axl*$^{-/-}$, *Mertk*$^{-/-}$, and *Axl*$^{-/-}$*Mertk*$^{-/-}$ double knockout mice sustained levels of infection similar to those of control animals. We also detected abundant viral RNA in tears, suggesting that virus might be secreted from lacrimal glands or shed from the cornea. This model provides a foundation for studying ZIKV-induced ocular disease, defining mechanisms of viral persistence, and developing therapeutic approaches for viral infections of the eye.

INTRODUCTION

ZIKV is a mosquito-transmitted flavivirus that is closely related to Dengue (DENV), West Nile (WNV), and yellow fever (YFV) viruses. Beyond the clinical syndromes of microcephaly, intrauterine growth restriction, and fetal demise, several clinical studies have observed eye malformations and pathology in neonates born to mothers infected with ZIKV during pregnancy (de Paula Freitas et al., 2016; McCarthy, 2016; Miranda et al., 2016; Sarno et al., 2016; Ventura et al., 2016a, 2016b). Manifestations of eye disease in newborns with ZIKV include chorioretinal atrophy, optic neuritis, bilateral iris colobomas, intraretinal hemorrhages, lens subluxation, and blindness (de Paula Freitas et al., 2016; Miranda et al., 2016; Ventura et al., 2016a, 2016b).

Viral infection in the eye can cause inflammation of uveal tissues (retina, choroid, iris, and ciliary body), also termed uveitis, which can lead to permanent vision loss if untreated (Niederkorn, 2006). In 2014, an Ebola virus (EBOV)-infected patient in the convalescent phase presented with uveitis. The aqueous humor of this patient's eye contained persistent EBOV RNA well after clearance of the virus in non-immune-privileged sites (Varkey et al., 2015). A subsequent study identified 57 EBOV survivors with uveitis, suggesting that infectious virus or viral RNA in the eye might have triggered this complication (Tiffany et al., 2016). Other animal models have suggested that some DNA viruses (e.g., ectromelia virus) might persist in the eye and recrudesce after immunosuppression (Sakala et al., 2015). ZIKV causes conjunctivitis in 10% to 15% of infected adults, and uveitis occurred in a patient several weeks after initial infection. Fluid sampled from the anterior chamber of this patient's eye contained viral RNA (Furtado et al., 2016), suggesting that ZIKV can replicate within the eye at some stage of its clinical syndrome.

ZIKV does not replicate efficiently in adult wild-type (WT) mice; this phenotype might be explained by the ability of ZIKV to antagonize human but not mouse STAT2, which is activated by signaling through the type I and type III interferon (IFN) receptors (Ashour et al., 2009; Grant et al., 2016). Accordingly, we and others have recently described models of ZIKV pathogenesis after congenital and adult infection in mice deficient in signaling

through the type I IFN receptor (Aliota et al., 2016; Lazear et al., 2016; Miner et al., 2016; Rossi et al., 2016). Mice lacking the type I IFN receptor (*Ifnar1*$^{-/-}$ mice) developed neuroinvasive disease after ZIKV infection, which caused death in younger animals, although a fraction of older adult mice survived infection. Infection of *Ifnar1*$^{-/-}$ females with a French Polynesian strain of ZIKV resulted in fetal demise and intrauterine growth restriction in *Ifnar1*$^{+/-}$ fetuses (Miner et al., 2016), but ocular pathology was not assessed.

Some flaviviruses are thought to attach to or enter target cells by interacting with TAM receptors (Tyro3, Axl, or Mertk) via their ligands, Gas6 and protein S, which bind to phosphatidylserine displayed on the surface of the virion. In vitro studies have suggested that TAM receptors can facilitate infection with WNV, DENV, and ZIKV either by promoting binding (Hamel et al., 2015; Meertens et al., 2012) or by activating TAM receptors (Bhattacharyya et al., 2013), which negatively regulate signaling through Ifnar1, resulting in a more permissive environment for replication. Recent focus has been placed on ZIKV infection and Axl, because it is expressed highly on neuroprogenitor cells (Nowakowski et al., 2016) and subtypes of trophoblasts (Tabata et al., 2016), which are key cellular targets of ZIKV.

Here, we evaluated whether ZIKV infects and injures the eyes of mice. Although we did not detect eye pathology in congenitally infected mice, ZIKV infected the iris, retina, and optic nerve of adult mice and caused conjunctivitis, panuveitis, and neuroretinitis without global photoreceptor abnormalities. Acute uveitis was associated with high levels of ZIKV RNA and infectious virus in the eye and detectable viral RNA in the tears and lacrimal glands. ZIKV RNA persisted within the eye through the convalescent stage, while infectious virus was cleared within 28 days. Although Axl and Mertk are expressed in eye tissues (Prasad et al., 2006; Valverde et al., 2004), infection studies in *Axl*$^{-/-}$ and *Mertk*$^{-/-}$ mice revealed no difference in ocular or brain infection, suggesting that these TAM receptors lack an essential entry or signaling role in these tissues. Our experiments establish that ZIKV infects specific target cells in different regions of the eye and provide a model for the development and testing of treatments for acute and persistent viral infections in the eye.

RESULTS

ZIKV Infection of the Eye with Viral RNA Shedding into Tears

ZIKV does not replicate efficiently in WT C57BL/6 mice, in part because ZIKV NS5 antagonizes human but not mouse STAT2 (Grant et al., 2016), which transmits signals downstream of Ifnar1, a component of the type I IFN receptor. To overcome this limitation, we treated mice with an anti-Ifnar1 blocking antibody (Lazear et al., 2016; Miner et al., 2016) and subcutaneously inoculated them with low-passage ZIKV contemporary clinical isolates, including strains from French Polynesia (H/PF/2013) and Brazil (Paraíba 2015). WT adult mice treated with anti-Ifnar1 monoclonal antibody (mAb) and inoculated with these ZIKV isolates do not develop clinically apparent disease, although viremia and infection of multiple organs occurs, including in immune-privileged sites such as the testes (Lazear et al., 2016). In comparison, *Ifnar1*$^{-/-}$ mice develop neuroinvasive infection, causing some of these animals to succumb to infection (Aliota et al., 2016; Lazear et al., 2016; Rossi et al., 2016). In anti-Ifnar1 mAb-treated animals, we detected RNA of ZIKV H/PF/2013 or Paraíba 2015 in the eye at day 2 after infection, which increased at day 6 (Figure 1A). Similar results were obtained after infection of *Ifnar1*$^{-/-}$ mice with Paraíba 2015, with high intraocular levels of ZIKV RNA accumulating by day 7 (Figure 1B).

Given the data on persistence of eye infection in humans after infection with EBOV and ZIKV (Furtado et al., 2016; Varkey et al., 2015), we assessed infection in mice 28 days after inoculation. Notably, ZIKV RNA persisted in several tissues, including the eyes, brain, spleen, and other organs, long after the virus was cleared from serum (Figure 1C and data not shown). During the 2015 EBOV epidemic, there was concern for person-to-person spread through ocular secretions, including tears (Varkey et al., 2015). As such, we next tested whether ZIKV RNA was present in tear fluid after eye lavage of infected animals with 10 μl of PBS. We detected ZIKV RNA in tear fluid ($\sim 3 \times 10^2$ focus-forming units [FFUs] equivalents per mL) and in the lacrimal gland ($\sim 2.4 \times 10^3$ FFU equivalents per mL) on day 7 after infection (Figures 1D and 1E), suggesting that infectious virus, viral RNA, or ZIKV-infected cellular debris were present in ocular secretions.

To determine whether ZIKV RNA in eyes (day 7 and day 28) and tears (day 7) was infectious, we inoculated AG129 mice via an intraperitoneal route with ocular homogenates or tear fluid; these mice were utilized because they lack receptors for both type I and II IFN signaling and are highly vulnerable to ZIKV infection even after inoculation with 1 plaque forming unit (PFU) (Aliota et al., 2016), which we confirmed (data not shown). Inoculation with eye homogenates obtained from *Ifnar1*$^{-/-}$ mice infected with Paraíba 2015 at day 7 resulted in death of AG129 mice, which occurred uniformly by day 10 (Figure 2A). In contrast, mice inoculated with eye homogenates from day 28 or tears from day 7 did not develop signs of ZIKV infection (Figure 2A and data not shown). These data suggest that infectious virus was not produced in the eye after the acute phase of infection. We observed conjunctivitis in *Ifnar1*$^{-/-}$ mice infected with ZIKV Paraíba 2015, although this occurred in some but not all animals (Figure 2B and data not shown). In the AG129 mice inoculated with day 7 eye homogenates, we observed greater ocular pathology, including severe conjunctivitis with extraocular exudate in all animals, compared to milder disease in mice receiving a similar dose of the parental ZIKV Paraíba 2015 (Figures 2B and 2C).

Nonetheless, we observed similar titers in the spleen, brain, and eyes of AG129 mice inoculated with either parental or eye-derived virus (Figure 2D). We considered whether the severe pathology seen with the eye-derived virus might be due to a virus adaptation that enhances ocular tropism or injury. To evaluate this hypothesis, we performed next-generation sequencing of eye-, spleen-, and brain-derived virus from ZIKV-infected *Ifnar1*$^{-/-}$ animals (Figure S1 and Table S1). Although we did not identify any substitutions that were absent in the inoculating virus, we observed a large increase in the frequency of a single NS2A nucleotide mutation (C→T at genome position 3,895, from ~10% to ~80% in all biological replicates and in all tissues tested) that resulted in an alanine to valine change.

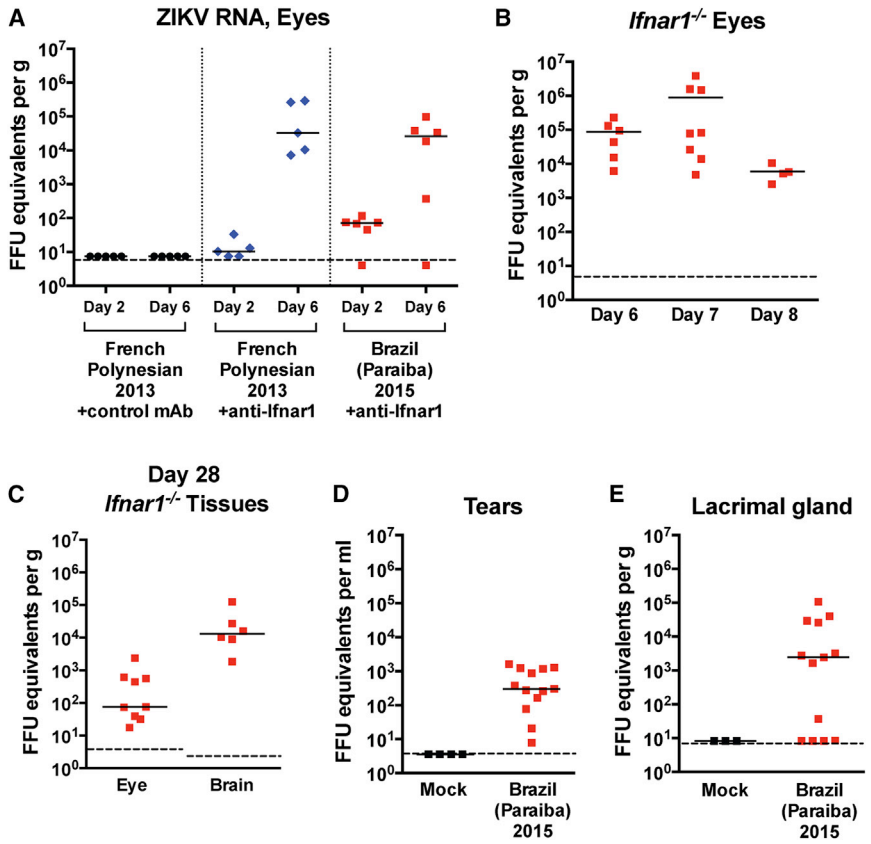

Figure 1. Viral Burden in the Eyes, Tears, and Lacrimal Gland of ZIKV-Infected Animals

4-week-old mice were infected with 10^3 FFUs of ZIKV Paraíba 2015. Viral burden was measured by qRT-PCR assay.

(A) Viral burden in the eyes of WT mice on days 2 and 6 after infection with ZIKV Paraíba 2015 or H/PF/2013. Mice were treated with 2 mg of an anti-Ifnar1 or control mAb 1 day prior to infection.

(B) Viral burden in the eyes of Ifnar1$^{-/-}$ mice on days 6, 7, and 8 after infection with ZIKV Paraíba 2015.

(C) Viral burden in the eyes and brain of Ifnar1$^{-/-}$ mice on day 28 after infection with ZIKV Paraíba 2015.

(D) Viral RNA in tears of mock- and ZIKV-infected Ifnar1$^{-/-}$ mice on day 7 after infection with ZIKV Paraíba 2015.

(E) Viral RNA in the lacrimal gland of mock- and ZIKV-infected Ifnar1$^{-/-}$ mice on day 7 after infection with ZIKV Paraíba 2015.

Symbols are derived from individual animals and pooled from two or three independent experiments. Bars indicate the mean of 5 to 13 mice per group. Dotted lines represent the limit of sensitivity of the assay.

Axl and Mertk Are Not Required for ZIKV Infection of the Eye and Brain In Vivo

The TAM receptors (Tyro3, Axl, and Mertk) are a family of receptor tyrosine kinases whose ligands, Gas6 and protein S, bind to phosphatidylserine on the surface of apoptotic cells and enveloped viruses (Meertens et al., 2012). Because prior studies have suggested that Axl might act as an attachment or entry receptor for ZIKV (Hamel et al., 2015; Nowakowski et al., 2016; Savidis et al., 2016) and TAM receptors are expressed in multiple cell types in the eye (Prasad et al., 2006; Valverde et al., 2004), we hypothesized Axl or its related TAM receptor, Mertk, might be required for efficient ZIKV replication in ocular tissues. Unexpectedly, *Axl*$^{-/-}$, *Mertk*$^{-/-}$, and *Axl*$^{-/-}$*Mertk*$^{-/-}$ double knockout (DKO) mice that were treated with anti-Ifnar1 mAb exhibited similar levels of ZIKV RNA in the serum, spleen, brain, and eyes on day 6 after infection as compared to similarly treated WT control animals (Figures 3A–3D). Thus, in mice deficient in IFN signaling, Axl and Mertk are not required for ZIKV infection in several tissues, including the eyes.

ZIKV Infects the Eyes and Brain of Young WT Mice

Congenital ZIKV infection in humans causes ocular pathology including optic neuritis, retinal mottling, and chorioretinal atrophy (de Paula Freitas et al., 2016; Miranda et al., 2016; Ventura et al., 2016a, 2016b). This could be a consequence of direct eye infection or it might be due to secondary brain defects that disrupt eye development. To test whether ocular pathology occurs in mice infected with ZIKV in utero, we modified a previously described congenital infection model with *Ifnar1*$^{-/-}$ dams and *Ifnar1*$^{+/+}$ sires such that *Ifnar1*$^{+/-}$ fetuses develop intrauterine growth restriction and brain injury but not isolated microcephaly (Miner et al., 2016). After infection with ZIKV Paraíba 2015 at embryonic day (E) 6.5 or E12.5 (equivalent to the late first and second trimesters, respectively), we confirmed the presence of ZIKV RNA in the heads of infected *Ifnar1*$^{+/-}$ fetuses 6 to 7 days later (E13.5 and E18.5) by qRT-PCR (Figure 4A). As reported previously (Miner et al., 2016), substantive demise of *Ifnar1*$^{+/-}$ fetuses was observed by E13.5 after ZIKV infection of *Ifnar1*$^{-/-}$ dams at E6.5, which precluded analysis of fetal ocular tissues. However, fetuses treated with an anti-Ifnar1 mAb survived ZIKV infection on E6.5 but did not show ocular abnormalities by histological analysis (Figure 4B). When *Ifnar1*$^{-/-}$ dams were inoculated later in gestation (E12.5), intrauterine growth restriction occurred without fetal demise (Figure 4C). Again, no histologically apparent pathology or developmental abnormality was observed at E18.5 in the eyes of *Ifnar1*$^{+/-}$ fetuses (Figure 4D).

Because we observed delayed clearance of ZIKV from the eyes of adult mice (see Figure 1C), we tested for viral persistence in the eyes of congenitally infected pups on postnatal day 8. After testing five different experimental conditions, including infection of anti-Ifnar1 mAb-treated pregnant WT mice at different gestational dates with ZIKV H/PF/2013 or Paraíba 2015, we detected viral RNA in eyes of only 2 of 41 congenitally infected animals (Figure 4E). These results suggest that ZIKV might not infect the eyes of fetuses efficiently in this model of in utero infection, even though it crosses the placenta (Miner et al., 2016). In contrast, postnatal infection of WT mice with ZIKV on day 8 after

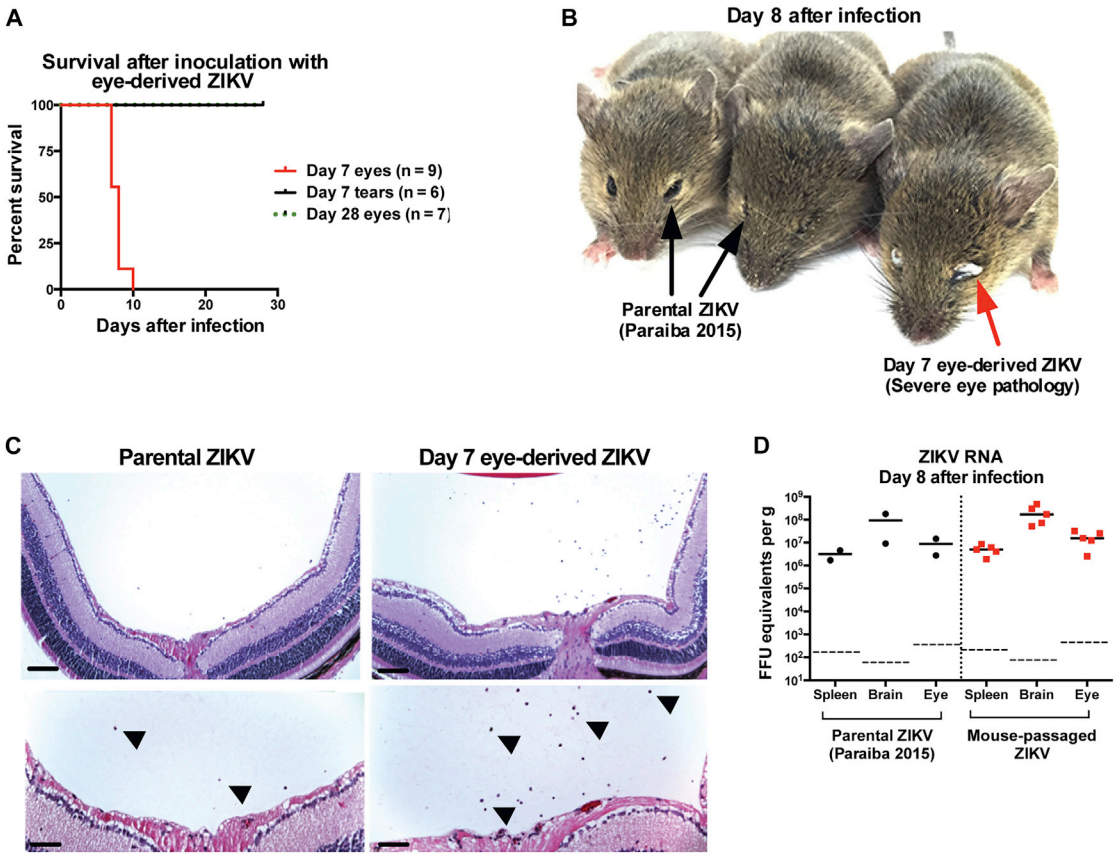

Figure 2. Survival and Viral Burden in AG129 Mice Inoculated with Tears and Eye Homogenate Derived from Infected Ifnar1$^{-/-}$ Mice

4-week-old AG129 mice were inoculated intraperitoneally with 10^4 FFUs of parental ZIKV Paraíba 2015 or eye-derived virus obtained from Ifnar1$^{-/-}$ mice.

(A) Kaplan-Meier survival curve in mice inoculated with day 7 or day 28 eye homogenates from Ifnar1$^{-/-}$ mice or 10 μL of tears obtained 7 days after ZIKV infection of Ifnar1$^{-/-}$ mice.

(B) A representative photograph demonstrating gross ocular pathology and exudate in mice inoculated with 10^4 FFUs of parental ZIKV Paraíba 2015 or eye-derived virus obtained from Ifnar1$^{-/-}$ mice.

(C) Representative H&E-stained eye sections from AG129 mice infected with parental and eye-derived ZIKV. Black arrowheads indicate inflammatory cell infiltrates in the posterior region of the eye. Scale bars represent 100 μm for upper panels and 75 μm for lower panels.

(D) Viral burden assessed by qRT-PCR assay in the spleen, brain, and eyes of AG129 mice inoculated with 10^4 FFUs of parental ZIKV Paraíba 2015 or eye-derived virus obtained from Ifnar1$^{-/-}$ mice.

Symbols are derived from individual animals and pooled from two or three independent experiments. Bars indicate the mean of two to five mice per group. Dotted lines represent the limit of sensitivity of the assay. See also Figure S1.

birth caused a subset of animals to become moribund, and ZIKV RNA was detected readily in the spleen, brain, and eyes 8 days later (Figure 4F). These data establish that ZIKV infection of the eye occurs in young mice even with intact type I IFN signaling. Examination of the brains of these postnatally infected animals revealed apoptosis (as detected by activated caspase-3 staining) in several CNS regions, including the optic tract, lateral geniculate nucleus, and the visual cortex, all components of the visual processing pathway (Figures 4G and 4H).

Anatomically, the eye is divided into the anterior (cornea, iris, ciliary body, and lens) and posterior (vitreous, retina, retinal pigment epithelium, choroid, and optic nerve) compartments, each with specialized cells and functions (Figure 5A). We evaluated the extent of eye injury in *Ifnar1*$^{-/-}$ or anti-Ifnar1 mAb-treated adult animals infected with ZIKV. Histopathological analysis revealed TUNEL-positive cells in the neurosensory retina (Figure 5B, white punctate staining). H&E staining showed anterior uveitis with infiltration of inflammatory cells in the anterior chamber (Figure 5C, upper right panel). The posterior eye also exhibited evidence of uveitis with inflammatory cell infiltration, exudate, and debris in the vitreous humor (Figure 5C, lower right panel). We next assessed the fundus of the eye for gross structural damage by using biomicroscopic and fundoscopic examination; no differences were observed between mock- and ZIKV-infected *Ifnar1*$^{-/-}$ or anti-Ifnar1 mAb-treated mice on day 7 (Figure S2 and data not shown). These experiments suggest that ZIKV infection does not induce significant pan-retinal abnormalities. Fluorescein angiography in ZIKV-infected *Ifnar1*$^{-/-}$ mice also revealed no evidence of vascular leakage or intraretinal hemorrhages (Figure S2). Thus, ZIKV infection in adult mice causes panuveitis without major structural damage or effects on vascular permeability.

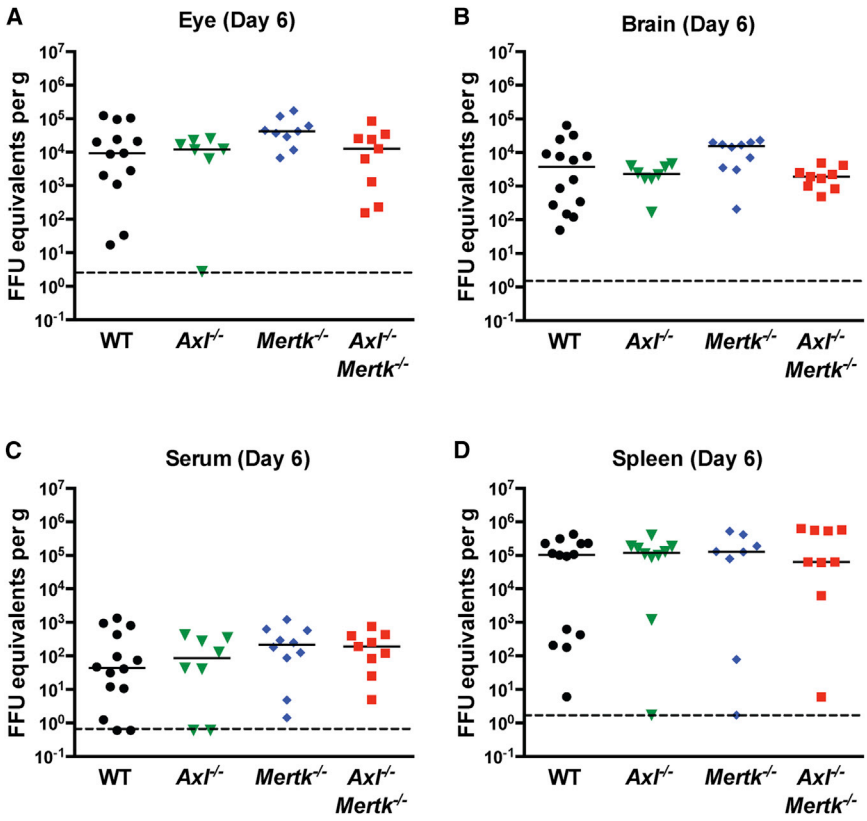

Figure 3. Viral Burden in WT, Axl$^{-/-}$, Mertk$^{-/-}$, or Axl$^{-/-}$Mertk$^{-/-}$ DKO Mice

4-to-6-week-old WT, Axl$^{-/-}$, Mertk$^{-/-}$, or Axl$^{-/-}$Mertk$^{-/-}$ DKO mice were treated with 2 mg of anti-Ifnar1 mAb 1 day prior to subcutaneous infection with 10^3 FFUs of ZIKV Paraíba 2015. On day 6 after infection, viral burden was measured by qRT-PCR in the eye (A), brain (B), serum (C), and spleen (D).

Symbols are derived from individual animals and pooled from two independent experiments. Bars indicate the mean of 8 to 14 mice per group. Dotted lines represent the limit of sensitivity of the assay. Data were analyzed by Kruskal-Wallis one-way ANOVA with a Dunn's multiple comparison test ($p > 0.1$ for comparison of all genotypes to the WT in all tissues).

To determine whether ZIKV infection of the eye caused functional deficits, we performed ex vivo electroretinography (ERG), which measures the transmission of light by photoreceptor cells. ERG testing of dissected eyes from *Ifnar1*$^{-/-}$ mice on day 7 after ZIKV infection revealed no apparent defects in photoreceptor function (Figures S3A– S3D). Similar results were obtained on days 7, 14, and 28 in ZIKV-infected WT mice treated with anti-Ifnar1 mAb (Figures S3E–S3H and data not shown). Thus, ZIKV infection and persistence in the eye does not cause global photoreceptor dysfunction. This ERG evaluation, however, does not rule out mild or focal defects in photoreceptor function or whether neuronal dysfunction of the inner retina and damage to the optic nerve, optic tract, or visual cortex occurs, any of which could result in blindness or selective visual field defects.

We evaluated the cellular tropism of ZIKV in the eye. Initially, we performed microdissection and measured ZIKV RNA levels in different compartments of the eye on day 7 after infection (Figure 6A). We included analysis of the anterior (cornea, iris, and lens) and posterior (neurosensory retina, retinal pigment epithelium/choroid complex, and optic nerve) chambers (see Figure 3B). ZIKV RNA was detected in all eye regions, with ~100-fold higher levels in the retinal pigment epithelium/choroid complex than in the optic nerve ($p < 0.05$, Figure 6A). To confirm these findings, eyes were collected at 6 to 8 days after inoculation and assessed for viral RNA by in situ hybridization (ISH). Mock-infected animals stained for ZIKV RNA and infected animals stained with a negative control probe against a bacterial gene had no staining in the cornea, optic nerve, or retina (Figure 6B and data not shown). In comparison, abundant ZIKV RNA was apparent in the bipolar and ganglion cell neurons of the neurosensory retina (Figure 6C, upper panel), the optic nerve (Figure 6C, middle panel), and the cornea of infected animals (Figure 6C, lower panel).

DISCUSSION

Understanding the consequences of ocular infection by viruses has become of greater concern because of the potential implications related to viral persistence and spread. Case reports of human patients infected with herpes simplex virus-1 (HSV-1), EBOV, ZIKV, and WNV suggest that some viruses have the capacity to cause significant acute ocular pathology, including uveitis and keratitis (Chong et al., 2004; Furtado et al., 2016; Kuchtey et al., 2003; Varkey et al., 2015). Since ZIKV does not efficiently infect WT mice, we tested whether it targets the eyes of mice by using a published model of ZIKV pathogenesis in adult animals deficient in type I IFN immunity as well as in immunocompetent neonatal mice and fetuses. Although we did not observe evidence of congenital ocular disease, which has been described in humans (de Paula Freitas et al., 2016; McCarthy, 2016; Ventura et al., 2016a, 2016b), ZIKV infected the eye and caused conjunctivitis and severe uveitis in immunodeficient adult mice. RNA ISH and virological analysis revealed that ZIKV infects the cornea, vascularized choroid, bipolar and ganglion layers of the retina, and optic nerve. Although the mechanism by which ZIKV causes eye disease remains undefined, our studies provide an animal model that can be used to define host factors that restrict pathogenesis and test candidate antiviral therapies directly within the eye.

The most common form of ZIKV-induced ocular disease is conjunctivitis, which occurs in 10% to 15% of patients, but whether conjunctivitis is a direct consequence of ZIKV infection of the eye is not known. In contrast, ZIKV-induced uveitis is less common, although it has been described in humans (Furtado et al., 2016). How ZIKV triggers uveitis remains uncertain,

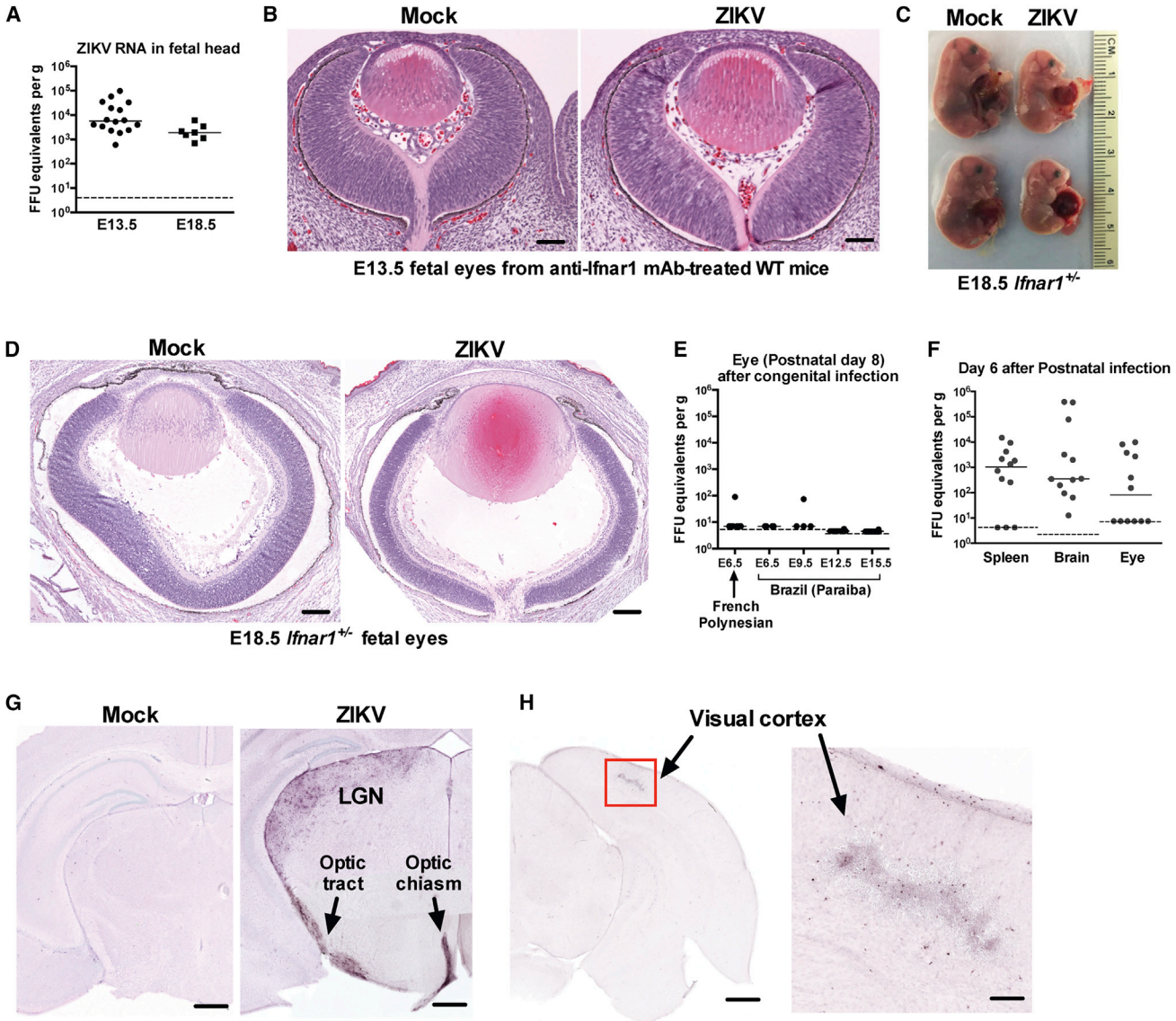

Figure 4. Histology and Viral Burden in the Eye after Congenital and Early Postnatal Infection with ZIKV

(A–E) Pregnant WT mice treated with 2 mg of an anti-Ifnar1 mAb or Ifnar1$^{-/-}$ mice were infected subcutaneously with 10^3 FFUs of ZIKV Paraíba 2015 WT, except where the French Polynesian strain is indicated in (E).

(A) Viral burden was assessed by qRT-PCR on E13.5 in WT fetuses or E18.5 in Ifnar1$^{+/-}$ fetuses after E6.5 and E12.5 infection, respectively.

(B) Representative H&E-stained eye sections from mock- and ZIKV-infected WT fetuses on E13.5.

(C) A representative photograph demonstrating the average size of mock- and ZIKV-infected Ifnar1$^{+/-}$ fetuses on E18.5.

(D) Representative H&E-stained eye sections from mock- and ZIKV-infected Ifnar1$^{+/-}$ fetuses on E18.5. The retinal detachment in the mock-infected sample is a commonly seen artifact of sectioning.

(E) Viral burden in the eyes of WT pups on postnatal day 8 after in utero ZIKV infection of anti-Ifnar1 mAb-treated WT pregnant dams at the indicated gestational date with the indicated strain.

(F–H) WT pups were inoculated subcutaneously on postnatal day 8 with 10^3 FFUs of ZIKV Paraíba 2015 WT and harvested 6 days later.

(F) Viral burden was assessed by qRT-PCR in the spleen, brain, and eye.

(G) Activated caspase-3 staining of mock- (left panel) and ZIKV-infected (right panel) WT pup brains, including the visual pathway (optic chiasm, optic tract, and lateral geniculate nucleus [LGN]). The image was generated by combining images of several coronal sections in the same animal into a single merged figure.

(H) Activated caspase-3 staining of a ZIKV-infected WT pup brain highlighting apoptosis in the visual cortex (red box) at higher magnification (right panel).

Results are from at least two or three independent experiments with 7 to 16 animals for viral burden analysis and 2 to 4 mice for histological analysis. Scale bars represent 25 μm for (B), 60 μm for (D), 500 μm for (G), and 1 mm for (H). Dotted lines represent the limit of sensitivity of the assay.

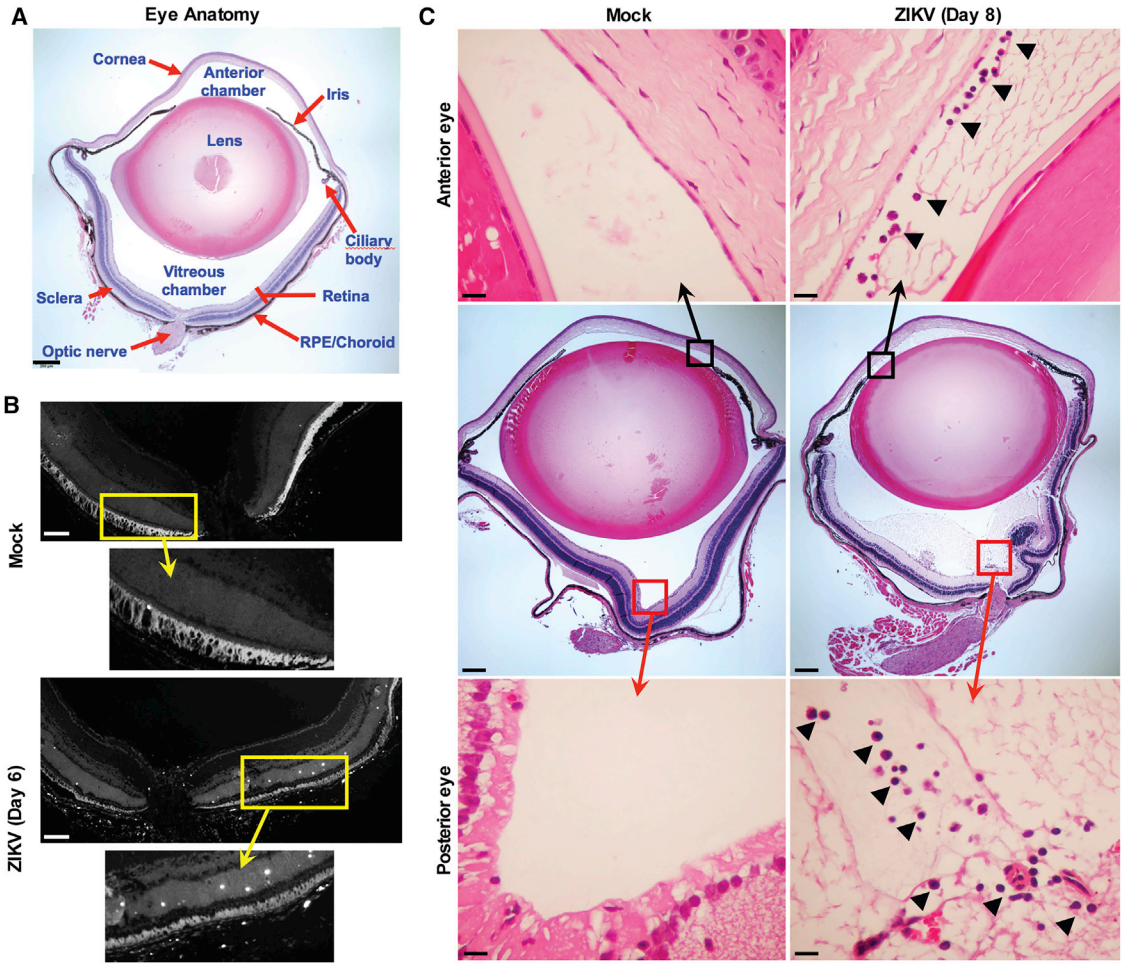

Figure 5. Histology of the Eye in Adult Ifnar1$^{-/-}$ Mice after Infection with ZIKV

4-to-8-week-old Ifnar1$^{-/-}$ mice were inoculated subcutaneously with 10^3 FFUs of ZIKV Paraíba 2015. On days 6 or 8 after infection, eyes were harvested.

(A) Anatomy of an uninfected eye, demonstrating anterior (cornea, lens, iris, and ciliary body) and posterior (sclera, retina, retinal pigment epithelium/choroid, and optic nerve) structures.

(B) TUNEL staining of the neurosensory retina of a mock (upper panel) or ZIKV-infected animal on day 6 (lower panel). Regions shown in higher magnification are indicated by a yellow box and arrow. Scale bars represent 100 μm.

(C) H&E-stained eye sections from mock- (left panels) and ZIKV-infected animals on day 8 (right panels). Regions shown in higher magnification are indicated by a box and displayed in the upper and lower panels. Black arrowheads indicate inflammatory cell infiltrates in the anterior (upper panels) and posterior (lower panels) chambers of the eye. Scale bars represent 250 μm (middle panels) and 25 μm (upper and lower panels).

The data and images are representative of two independent experiments with two to four animals per group. See also Figures S2 and S3.

although inflammatory cell recruitment might contribute to this, according to our histological findings. Direct infection of the eye might cause inflammation as a consequence of virus-induced cell death, cytokine production, and/or leukocyte recruitment. Alternatively, intracellular or extracellular viral RNA can act as a pathogen-associated molecular pattern (PAMP) and activate inflammatory responses via stimulating pattern recognition receptors (e.g., Toll-like or Rig-I-like receptors), even in the absence of infectious virus. In humans with EBOV- and ZIKV-induced uveitis, viral RNA was detectable within the intraocular fluid. We found that mice infected with ZIKV had no infectious virus in the eye by day 28, even though high levels of ZIKV RNA were present. Consistent with this observation, there is extensive literature describing WNV-induced ocular disease in humans, including uveitis, chorioretinitis, and retinal artery occlusion (Hershberger et al., 2003; Kaiser et al., 2003; Kuchtey et al., 2003). Neurotropic flaviviruses might first invade the brain, then infect the optic tract, and later transit in a retrograde direction into the eye along the optic nerve. Alternatively, ocular infection might result from hematogenous spread of virus across the blood-retinal barrier. Additional studies are needed to define the precise mechanisms of ocular invasion by ZIKV.

ZIKV infects both the eyes and testes in humans and in animal models (Lazear et al., 2016; Musso et al., 2015), suggesting that immune-privileged organs might support replication even weeks after resolution of viremia and clinical symptoms. Hepatitis C virus, a related *Flaviviridae* family member, can infect the human cornea (Lee et al., 2001) and is transmitted by corneal

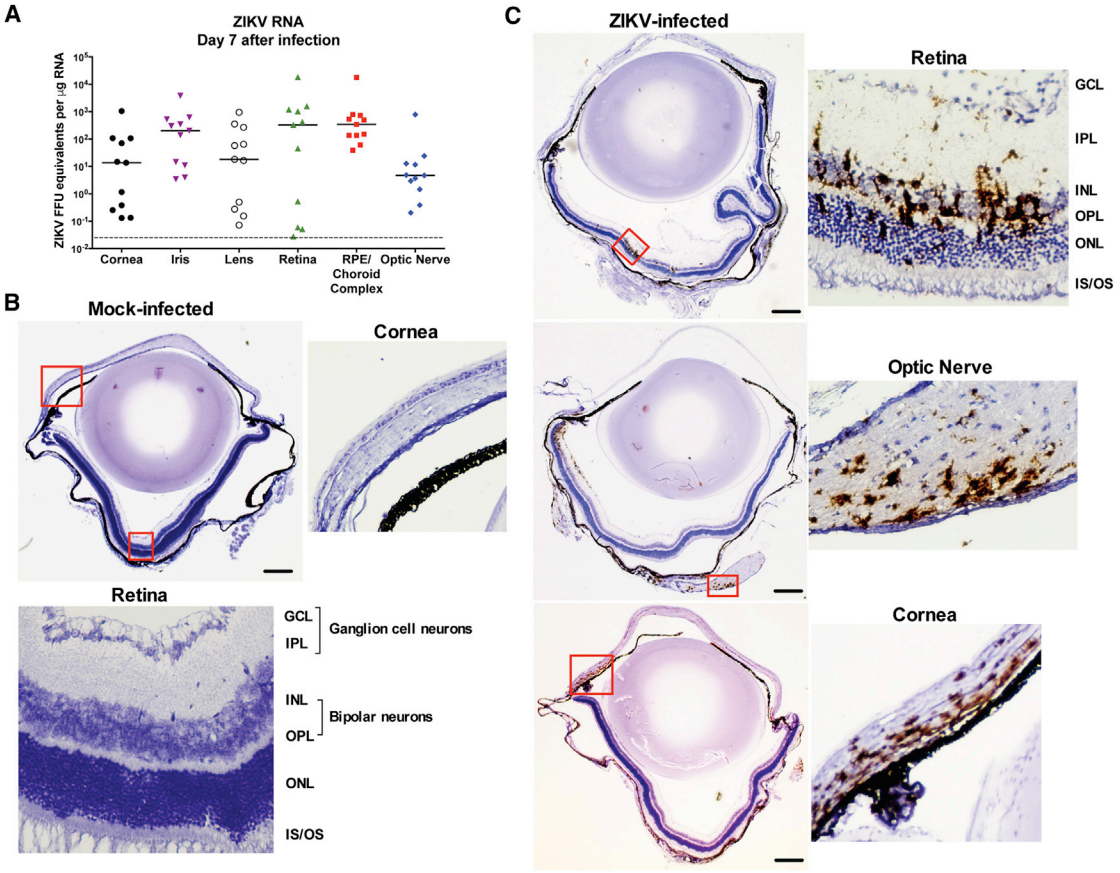

Figure 6. Viral Burden and Localization in the Anterior and Posterior Regions of the Eye

4-to-8-week-old Ifnar1$^{-/-}$ mice were inoculated subcutaneously with 10^3 FFUs of ZIKV Paraíba 2015. Eyes were harvested for microdissection and quantitation of ZIKV RNA by qRT-PCR (day 7) or for ZIKV RNA detection by ISH (day 6 or 8).

(A) Viral burden in the microdissected cornea, iris, lens, retina, retinal pigment epithelium/choroid, and optic nerve on day 7 after infection. Symbols are derived from individual animals and pooled from two independent experiments. Bars indicate the mean of 8 to 14 mice per group. Dotted lines represent the limit of sensitivity of the assay. Data were analyzed by Kruskal-Wallis one-way ANOVA with a Dunn's multiple comparison test ($p > 0.05$ only for samples from optic nerve compared to RPE/choroid complex).

(B and C) RNA ISH with a ZIKV-specific probe to stain eye sections of mock- (B) or ZIKV-infected (C) Ifnar1$^{-/-}$ mice. Red boxes indicate regions shown at higher magnification in adjacent panels. High-magnification views in (B) indicate regions of the cornea (right panel) and retina (bottom panel). High-magnification views in (C) show regions of the retina (right panel), optic nerve (middle panel), and cornea (lower panel). ISH data are representative of two independent experiments with at least two animals per group. Scale bar represents 200 μm.

transplantation (Tugwell et al., 2005). Given that ZIKV has capacity to infect the cornea of mice, human studies might be needed to confirm whether ZIKV analogously infects the human cornea. If corneal infection by ZIKV were established in humans, then widespread ocular infection during epidemics could necessitate testing by eye banks to ensure that ZIKV is not present in the corneas of infected donors.

Congenital ocular disease caused by ZIKV might be due to direct targeting of cells in the fetal eye. Alternatively, it could occur as part of a neurodevelopmental defect, which is seen in microcephaly cases even in the absence of an infectious cause (Derbent et al., 2004). Although a recent study suggested ocular pathology was present in SJL mouse pups that were infected with ZIKV in utero, histological characterization of their eyes was not demonstrated (Cugola et al., 2016). We did not observe histological abnormalities of the eyes of congenitally infected *Ifnar1*$^{+/-}$ fetuses from C57BL/6 *Ifnar1*$^{-/-}$ dams. Studies with other mouse and non-human primate models are needed to clarify the requirements and basis for ZIKV-induced congenital ocular disease.

TAM receptors might enhance attachment and entry of flaviviruses, including ZIKV (Hamel et al., 2015; Meertens et al., 2012; Savidis et al., 2016). This hypothesis has been strengthened by a correlation between levels of Axl expression and vulnerability of certain neuronal subtypes to ZIKV infection (Nowakowski et al., 2016). However, our studies in *Axl*$^{-/-}$, *Mertk*$^{-/-}$, and *Axl*$^{-/-}$*Mertk*$^{-/-}$ mice revealed no effect of a loss of expression of these TAM receptors on ZIKV replication, suggesting that Axl and Mertk are not required for CNS or ocular infection in mice. These results are analogous to prior studies with WNV, in which an absence of Axl and/or Mertk paradoxically resulted in enhanced infection in the brain, which was due in part to

alterations in the permeability of endothelial cells lining the blood-brain barrier (Miner et al., 2015). Our data do not exclude the possibility that Axl might still act as an entry factor for ZIKV in specific cells in other tissue compartments (e.g., trophoblasts in the placenta or subsets of neurons in the CNS).

In summary, we have described a mouse model of ocular disease that demonstrates ZIKV tropism in specific regions of the eye, panuveitis, shedding of viral RNA into tears, and persistence in immunodeficient adult mice. We have also confirmed that ZIKV infects the eye of immunocompetent neonatal WT mice. Studies are planned to define the cellular mechanisms by which ZIKV invades and infects the eye and results in inflammation. Further analysis of the host and virus factors that facilitate ocular infection and mechanisms of immune-mediated clearance could lead to interventions that enhance elimination of viruses from immune-privileged sites, including the eye.

EXPERIMENTAL PROCEDURES

Ethics Statement

This study was carried out in accordance with the recommendations in the Guide for the Care and Use of Laboratory Animals of the NIH. The protocols were approved by the institutional animal care and use committee at the Washington University School of Medicine (assurance number A3381-01). Inoculations were performed under anesthesia induced and maintained with ketamine hydrochloride and xylazine, and all efforts were made to minimize animal suffering.

Viruses and Titration

The ZIKV strain H/PF/2013 (French Polynesia, 2013) was provided by the Arbovirus Branch of the Centers for Disease Control and Prevention with permission (X. de Lamballerie, Aix Marseille Université) (Baronti et al., 2014). The ZIKV strain Paraíba 2015 (Brazil, 2015) was provided by Steve Whitehead (NIH). ZIKV stocks were propagated in Vero cells and titrated by focus-forming assay (FFA) as previously described (Lazear et al., 2016; Miner et al., 2016).

Mouse Experiments

Ifnar1$^{-/-}$ mice (Hwang et al., 1995) were backcrossed onto a C57BL/6 background. *Axl*$^{-/-}$, *Mertk*$^{-/-}$, and *Axl*$^{-/-}$*Mertk*$^{-/-}$ mice have been published (Lu and Lemke, 2001) and were backcrossed for ten generations. Mice were bred in a specific-pathogen-free facility at Washington University or purchased (WT animals) from Jackson Laboratories. In some experiments, WT mice were treated with 2 mg of an anti-Ifnar1 blocking mouse mAb (MAR1-5A3) or isotype control mouse mAb (GIR-208; Leinco Technologies) (Sheehan et al., 2006, 2015) by intraperitoneal injection prior to infection with ZIKV. 4- to 8-week-old mice were inoculated with ZIKV by subcutaneous (footpad) route with 10^3 FFU in 50 μL of PBS. Mice were sacrificed at day 2, 6, 7, 8, or 28, depending on the experimental design, and organs were harvested. To study congenital infection, anti-Ifnar1 mAb-treated WT pregnant mice were infected with the indicated strains of ZIKV at E6.5, E9.5, E12.5, or E15.5, and tissues were harvested at postnatal day 8. For some experiments, pregnant *Ifnar1*$^{-/-}$ females carrying *Ifnar1*$^{+/-}$ fetuses were infected on E12.5. *Ifnar1*$^{+/-}$ fetal tissues were harvested on E18.5 as previously described (Miner et al., 2016). For studies in neonatal WT animals, mice were inoculated subcutaneously on postnatal day 7 or 8 and then tissues were harvested 6 days later and analyzed for the presence of viral RNA. For comparison of parental (Paraíba 2015) and mouse-passaged ZIKV, AG129 mice (van den Broek et al., 1995) were inoculated via an intraperitoneal route with 10^4 FFU of parental ZIKV or an equivalent dose (based on viral RNA) from eye homogenates collected from *Ifnar1*$^{-/-}$ mice on day 7 or day 28 after ZIKV infection. Alternatively, AG129 mice were inoculated via an intraperitoneal route with 10 μL of tears (diluted in 150 μL of PBS) collected from *Ifnar1*$^{-/-}$ mice on day 7 after infection with ZIKV (Paraíba 2015).

Measurement of Viral Burden

Tissues were weighed and homogenized with zirconia beads in a MagNA Lyser instrument (Roche Life Science) in 250 μL or 500 μL of PBS. Tissue samples and serum from ZIKV-infected mice were extracted with the RNeasy Mini Kit (tissues) or the Viral RNA Mini Kit (serum) (QIAGEN). ZIKV RNA levels were determined by one-step qRT-PCR on an ABI 7500 Fast Instrument using standard cycling conditions. Viral burden was expressed on a $\log_{10}$ scale as viral RNA equivalents per gram or per mL after comparison with a standard curve produced using serial 10-fold dilutions of ZIKV RNA. A published primer set was used to detect ZIKV RNA (Lanciotti et al., 2008; Miner et al., 2016).

Tears and Lacrimal Gland Collection

ZIKV-infected mice were euthanized on day 7 after infection. Tear fluid from both eyes was collected after gentle lavage with 10 μL of PBS using FP plus multiflex tips (Fisher Scientific). Intact lacrimal gland lobules were isolated by dissection.

TUNEL Staining

Cell death in the neurosensory retina of *Ifnar1*$^{-/-}$ mice was assessed 7 days after ZIKV infection by TUNEL staining. In brief, paraffin sections of eyes from ZIKV-infected mice were pretreated with proteinase K and stained with an ApopTag Fluorescein In Situ Apoptosis Detection Kit (Millipore) according to the manufacturer's instructions. Images of the retina were collected and merged into a composite image.

Brain Sectioning and Immunostaining for Activated Caspase-3

After ZIKV infection, animals were anesthetized and perfused via intracardiac injection with 4% paraformaldehyde in Tris-HCl buffer. Brains were then sectioned at 70 μm with a vibratome and stained for activated caspase-3 as described previously (Miner et al., 2016).

RNA ISH

RNA ISH was performed with an RNAscope 2.5 (Advanced Cell Diagnostics) according to the manufacturer's instructions. In brief, formalin-fixed paraffin-embedded tissue sections were deparaffinized by incubation for 60 min at 60°C. Endogenous peroxidases were quenched with hydrogen peroxide for 10 min at room temperature. Slides were then boiled for 15 min in RNAscope Target Retrieval Reagents and incubated for 30 min in RNAscope Protease Plus before probe hybridization. The probe targeting ZIKV RNA was designed and synthesized by Advanced Cell Diagnostics (catalog no. 467771). Positive (targeting *plr2a* gene) and negative (targeting bacterial gene *dapB*) control probes also were obtained from Advanced Cell Diagnostics (312471 and 310043, respectively). Tissues were counterstained with Gill's hematoxylin and visualized with standard bright-field microscopy.

Data Analysis

All data were analyzed with GraphPad Prism software. For viral burden analysis, the $\log_{10}$ transformed titers and levels of viral RNA were analyzed by the Mann-Whitney test or Kruskal-Wallis one-way ANOVA. A p value of < 0.05 indicated statistically significant differences.

SUPPLEMENTAL INFORMATION

Supplemental Information includes Supplemental Experimental Procedures, three figures, and one table and can be found with this article online at http://dx.doi.org/10.1016/j.celrep.2016.08.079.

AUTHOR CONTRIBUTIONS

J.J.M. and A.M.S. performed infections, tissue harvests, RNA isolation, qRT-PCR analysis, and some of the histological analysis. A.Sene performed ERG, fundoscopy, fluorescein angiography, TUNEL staining, and some of the histological analysis. A.Sene and N.B. dissected lacrimal glands and eye regions and collected tears. J.M.R. and A.M.S. performed all RNA ISH experiments. J.G. performed the ZIKV French Polynesian strain infection and

harvest. A.Santeford performed tissue sectioning and histological analysis. F.M. and K.N. performed histological analysis of the brain. J.W., C.R., and G.D.E. performed the next-generation sequencing and analysis. A.Sene wrote parts of the initial draft. J.J.M. wrote the initial complete draft of the manuscript. J.J.M., M.S.D., and R.S.A. edited the manuscript. J.J.M, M.S.D, and R.S.A are corresponding authors. As a group, the corresponding authors shared responsibility for all data, figures, and text, determination of authorship, approval of content by authors, adherence to editorial policies, declaration of conflict of interests, and ensuring figures are representative of the original data. M.S.D. is the lead contact for journal communication and is the primary contact for reagent and resource sharing.

ACKNOWLEDGMENTS

This study was supported by grants from the NIH (R01 AI073755, R01 AI101400, and R01 AI104972 [to M.S.D.], R01 EY019287 [to R.S.A.], P30 EY02687 [Vision Core Grant], and R01 AI067380 [to G.D.E.]). R.S.A. also was supported by a Physician-Scientist Award from Research to Prevent Blindness, the Schulak Family Gift Fund for Retinal Research, and the Jeffrey Fort Innovation Fund. J.J.M. was supported by a Rheumatology Research Foundation Scientist Development Award. K.N. was supported by the Intellectual and Developmental Disabilities Research Center at Washington University (NIH/NICHD U54 HD087011). Additional funding comes from an unrestricted grant to the Department of Ophthalmology and Visual Sciences of Washington University School of Medicine from Research to Prevent Blindness. M.S.D. is a consultant for Inbios, Visterra, Sanofi, and Takeda Pharmaceuticals, is on the Scientific Advisory Boards of Moderna and OraGene, and is a recipient of research grants from Moderna, Sanofi, and Visterra.

Received: July 27, 2016
Revised: August 12, 2016
Accepted: August 25, 2016
Published: September 6, 2016

REFERENCES

Aliota, M.T., Caine, E.A., Walker, E.C., Larkin, K.E., Camacho, E., and Osorio, J.E. (2016). Characterization of lethal Zika virus infection in AG129 mice. PLoS Negl. Trop. Dis. *10*, e0004682.

Ashour, J., Laurent-Rolle, M., Shi, P.-Y., and García-Sastre, A. (2009). NS5 of dengue virus mediates STAT2 binding and degradation. J. Virol. *83*, 5408–5418.

Baronti, C., Piorkowski, G., Charrel, R.N., Boubis, L., Leparc-Goffart, I., and de Lamballerie, X. (2014). Complete coding sequence of zika virus from a French polynesia outbreak in 2013. Genome Announc. *2*, e00500–e00514.

Bhattacharyya, S., Zagórska, A., Lew, E.D., Shrestha, B., Rothlin, C.V., Naughton, J., Diamond, M.S., Lemke, G., and Young, J.A. (2013). Enveloped viruses disable innate immune responses in dendritic cells by direct activation of TAM receptors. Cell Host Microbe *14*, 136–147.

Chong, E.-M., Wilhelmus, K.R., Matoba, A.Y., Jones, D.B., Coats, D.K., and Paysse, E.A. (2004). Herpes simplex virus keratitis in children. Am. J. Ophthalmol. *138*, 474–475.

Cugola, F.R., Fernandes, I.R., Russo, F.B., Freitas, B.C., Dias, J.L.M., Guimarães, K.P., Benazzato, C., Almeida, N., Pignatari, G.C., Romero, S., et al. (2016). The Brazilian Zika virus strain causes birth defects in experimental models. Nature *534*, 267–271.

de Paula Freitas, B., de Oliveira Dias, J.R., Prazeres, J., Sacramento, G.A., Ko, A.I., Maia, M., and Belfort, R., Jr. (2016). Ocular findings in infants with microcephaly associated with presumed zika virus congenital infection in salvador, brazil. JAMA Ophthalmol. *134*, 529–535.

Derbent, M., Agras, P.I., Gedik, S., Oto, S., Alehan, F., and Saatçi, U. (2004). Congenital cataract, microphthalmia, hypoplasia of corpus callosum and hypogenitalism: report and review of Micro syndrome. Am. J. Med. Genet. A. *128A*, 232–234.

Furtado, J.M., Espósito, D.L., Klein, T.M., Teixeira-Pinto, T., and da Fonseca, B.A. (2016). Uveitis associated with zika virus infection. N. Engl. J. Med. *375*, 394–396.

Grant, A., Ponia, S.S., Tripathi, S., Balasubramaniam, V., Miorin, L., Sourisseau, M., Schwarz, M.C., Sánchez-Seco, M.P., Evans, M.J., Best, S.M., and García-Sastre, A. (2016). Zika virus targets human STAT2 to inhibit type I interferon signaling. Cell Host Microbe *19*, 882–890.

Hamel, R., Dejarnac, O., Wichit, S., Ekchariyawat, P., Neyret, A., Luplertlop, N., Perera-Lecoin, M., Surasombatpattana, P., Talignani, L., Thomas, F., et al. (2015). Biology of zika virus infection in human skin cells. J. Virol. *89*, 8880–8896.

Hershberger, V.S., Augsburger, J.J., Hutchins, R.K., Miller, S.A., Horwitz, J.A., and Bergmann, M. (2003). Chorioretinal lesions in nonfatal cases of West Nile virus infection. Ophthalmology *110*, 1732–1736.

Hwang, S.Y., Hertzog, P.J., Holland, K.A., Sumarsono, S.H., Tymms, M.J., Hamilton, J.A., Whitty, G., Bertoncello, I., and Kola, I. (1995). A null mutation in the gene encoding a type I interferon receptor component eliminates antiproliferative and antiviral responses to interferons alpha and beta and alters macrophage responses. Proc. Natl. Acad. Sci. USA *92*, 11284–11288.

Kaiser, P.K., Lee, M.S., and Martin, D.A. (2003). Occlusive vasculitis in a patient with concomitant West Nile virus infection. Am. J. Ophthalmol. *136*, 928–930.

Kuchtey, R.W., Kosmorsky, G.S., Martin, D., and Lee, M.S. (2003). Uveitis associated with West Nile virus infection. Arch. Ophthalmol. *121*, 1648–1649.

Lanciotti, R.S., Kosoy, O.L., Laven, J.J., Velez, J.O., Lambert, A.J., Johnson, A.J., Stanfield, S.M., and Duffy, M.R. (2008). Genetic and serologic properties of Zika virus associated with an epidemic, Yap State, Micronesia, 2007. Emerg. Infect. Dis. *14*, 1232–1239.

Lazear, H.M., Govero, J., Smith, A.M., Platt, D.J., Fernandez, E., Miner, J.J., and Diamond, M.S. (2016). A Mouse Model of Zika Virus Pathogenesis. Cell Host Microbe *19*, 720–730.

Lee, H.M., Naor, J., Alhindi, R., Chinfook, T., Krajden, M., Mazzulli, T., and Rootman, D.S. (2001). Detection of hepatitis C virus in the corneas of seropositive donors. Cornea *20*, 37–40.

Lu, Q., and Lemke, G. (2001). Homeostatic regulation of the immune system by receptor tyrosine kinases of the Tyro 3 family. Science *293*, 306–311.

McCarthy, M. (2016). Severe eye damage in infants with microcephaly is presumed to be due to Zika virus. BMJ *352*, i855.

Meertens, L., Carnec, X., Lecoin, M.P., Ramdasi, R., Guivel-Benhassine, F., Lew, E., Lemke, G., Schwartz, O., and Amara, A. (2012). The TIM and TAM families of phosphatidylserine receptors mediate dengue virus entry. Cell Host Microbe *12*, 544–557.

Miner, J.J., Daniels, B.P., Shrestha, B., Proenca-Modena, J.L., Lew, E.D., Lazear, H.M., Gorman, M.J., Lemke, G., Klein, R.S., and Diamond, M.S. (2015). The TAM receptor Mertk protects against neuroinvasive viral infection by maintaining blood-brain barrier integrity. Nat. Med. *21*, 1464–1472.

Miner, J.J., Cao, B., Govero, J., Smith, A.M., Fernandez, E., Cabrera, O.H., Garber, C., Noll, M., Klein, R.S., Noguchi, K.K., et al. (2016). Zika Virus Infection during Pregnancy in Mice Causes Placental Damage and Fetal Demise. Cell *165*, 1081–1091.

Miranda, H.A., 2nd, Costa, M.C., Frazão, M.A.M., Simão, N., Franchischini, S., and Moshfeghi, D.M. (2016). Expanded Spectrum of Congenital Ocular Findings in Microcephaly with Presumed Zika Infection. Ophthalmology *123*, 1788–1794.

Musso, D., Roche, C., Robin, E., Nhan, T., Teissier, A., and Cao-Lormeau, V.M. (2015). Potential sexual transmission of Zika virus. Emerg. Infect. Dis. *21*, 359–361.

Niederkorn, J.Y. (2006). See no evil, hear no evil, do no evil: the lessons of immune privilege. Nat. Immunol. *7*, 354–359.

Nowakowski, T.J., Pollen, A.A., Di Lullo, E., Sandoval-Espinosa, C., Bershteyn, M., and Kriegstein, A.R. (2016). Expression analysis highlights AXL as a candidate Zika virus entry receptor in neural stem cells. Cell Stem Cell *18*, 591–596.

Prasad, D., Rothlin, C.V., Burrola, P., Burstyn-Cohen, T., Lu, Q., Garcia de Frutos, P., and Lemke, G. (2006). TAM receptor function in the retinal pigment epithelium. Mol. Cell. Neurosci. *33*, 96–108.

Rossi, S.L., Tesh, R.B., Azar, S.R., Muruato, A.E., Hanley, K.A., Auguste, A.J., Langsjoen, R.M., Paessler, S., Vasilakis, N., and Weaver, S.C. (2016). Characterization of a novel murine model to study Zika virus. Am. J. Trop. Med. Hyg. *94*, 1362–1369.

Sakala, I.G., Chaudhri, G., Scalzo, A.A., Eldi, P., Newsome, T.P., Buller, R.M., and Karupiah, G. (2015). Evidence for persistence of ectromelia virus in inbred mice, recrudescence following immunosuppression and transmission to naïve mice. PLoS Pathog. *11*, e1005342.

Sarno, M., Sacramento, G.A., Khouri, R., do Rosário, M.S., Costa, F., Archanjo, G., Santos, L.A., Nery, N., Jr., Vasilakis, N., Ko, A.I., and de Almeida, A.R. (2016). Zika virus infection and stillbirths: a case of hydrops fetalis, hydranencephaly and fetal demise. PLoS Negl. Trop. Dis. *10*, e0004517.

Savidis, G., McDougall, W.M., Meraner, P., Perreira, J.M., Portmann, J.M., Trincucci, G., John, S.P., Aker, A.M., Renzette, N., Robbins, D.R., et al. (2016). Identification of Zika virus and Dengue virus dependency factors using functional genomics. Cell Rep. *16*, 232–246.

Sheehan, K.C., Lai, K.S., Dunn, G.P., Bruce, A.T., Diamond, M.S., Heutel, J.D., Dungo-Arthur, C., Carrero, J.A., White, J.M., Hertzog, P.J., et al. (2006). Blocking monoclonal antibodies specific for mouse IFN-alpha/beta receptor subunit 1 (IFNAR-1) from mice immunized by in vivo hydrodynamic transfection. J. Interferon Cytokine Res *26*, 804–819.

Sheehan, K.C., Lazear, H.M., Diamond, M.S., and Schreiber, R.D. (2015). Selective blockade of interferon-α and -β reveals their non-redundant functions in a mouse model of West Nile virus infection. PLoS ONE *10*, e0128636.

Tabata, T., Petitt, M., Puerta-Guardo, H., Michlmayr, D., Wang, C., Fang-Hoover, J., Harris, E., and Pereira, L. (2016). Zika virus targets different primary human placental cells, suggesting two routes for vertical transmission. Cell Host Microbe *20*, 155–166.

Tiffany, A., Vetter, P., Mattia, J., Dayer, J.-A., Bartsch, M., Kasztura, M., Sterk, E., Tijerino, A.M., Kaiser, L., and Ciglenecki, I. (2016). Ebola virus disease complications as experienced by survivors in Sierra Leone. Clin. Infect. Dis. *62*, 1360–1366.

Tugwell, B.D., Patel, P.R., Williams, I.T., Hedberg, K., Chai, F., Nainan, O.V., Thomas, A.R., Woll, J.E., Bell, B.P., and Cieslak, P.R. (2005). Transmission of hepatitis C virus to several organ and tissue recipients from an antibody-negative donor. Ann. Intern. Med. *143*, 648–654.

Valverde, P., Obin, M.S., and Taylor, A. (2004). Role of Gas6/Axl signaling in lens epithelial cell proliferation and survival. Exp. Eye Res. *78*, 27–37.

van den Broek, M.F., Müller, U., Huang, S., Aguet, M., and Zinkernagel, R.M. (1995). Antiviral defense in mice lacking both alpha/beta and gamma interferon receptors. J. Virol. *69*, 4792–4796.

Varkey, J.B., Shantha, J.G., Crozier, I., Kraft, C.S., Lyon, G.M., Mehta, A.K., Kumar, G., Smith, J.R., Kainulainen, M.H., Whitmer, S., et al. (2015). Persistence of Ebola virus in ocular fluid during convalescence. N. Engl. J. Med. *372*, 2423–2427.

Ventura, C.V., Maia, M., Bravo-Filho, V., Góis, A.L., and Belfort, R., Jr. (2016a). Zika virus in Brazil and macular atrophy in a child with microcephaly. Lancet *387*, 228.

Ventura, C.V., Maia, M., Travassos, S.B., Martins, T.T., Patriota, F., Nunes, M.E., Agra, C., Torres, V.L., van der Linden, V., Ramos, R.C., et al. (2016b). Risk factors associated with the ophthalmoscopic findings identified in infants with presumed zika virus congenital infection. JAMA Ophthalmol. *134*, 912–918.